Journal of Network Intelligence ©2026 ISSN 2414-8105
Taiwan Ubiquitous Information Volume **11**, Number **1**, February **2026**

Trace Element Detection of Rock Minerals Based on ICP-MS and Support Vector Machine

Meng Meng[1,*], Ze-Gang Lu[1], Hui-Long Song[1]

[1]Heilongjiang Provincial Seventh Geological Exploration Institute,
Suihua 152000, P. R. China
meng20180129@163.com, yuzebt@126.com, songhuilong_2004@163.com

Hui-Ping Pan[2]

[2]Center for International Education,
Philippine Christian University, Manila 1004, Philippine
panhuiping@sohu.com

[*]Corresponding author: Meng Meng

Received December 27, 2024, revised May 17, 2025, accepted August 28, 2025.

Abstract. *Trace element detection of rock minerals is of great importance in the fields of geology, mineral exploration and environmental science. In this paper, to address the problem that the relationship between rock minerals and trace elements in existing methods is nonlinear, which reduces the accuracy of detection, firstly, the microwave digestion method is used to convert the rock samples into solutions, and then the trace elements in rock minerals are directly determined by Inductively Coupled Plasma-Mass Spectrometry (ICP-MS). A correction equation is established to eliminate the polyatomic ionic interference produced by oxide ions on trace elements, thus obtaining the electrical signals of trace elements. Secondly, the electrical signal is denoised using improved wavelet transform and the decomposed signal is reconstructed in terms of energy distribution. Then the principal component analysis algorithm is used to eliminate the irrelevant signal variables, and on this basis, CNN is used to extract and fuse the important signal feature information, and then the Harris Hawk optimization algorithm is used to find the optimal SVM hyper-parameters to fit the relationship between the trace element content and the signal features, so as to complete the detection of trace elements in the rock minerals. The experimental outcome implies that the Relative Standard Deviation (RSD) of the offered approach was less than 9.6%, and the detection accuracy was improved by 5-12.5%, which indicated that the offered approach could improve the accuracy of modeling and effectively identify different types of trace elements.*
Keywords: Trace element detection; ICP-MS; Wavelet transform; Principal component analysis; Support vector machine.

---

1. **Introduction.** Geological rock minerals are polymers formed by a variety of elements, gradually formed during the internal movement of the earth's crust, it can be seen that the key to the production of geological rock minerals is geological action. There are different types of geological activities in different parts of China, and the geological application level is also very different, in order to ensure that mining is carried out smoothly and efficiently, it is necessary to pay attention to the detection and analysis of trace elements of geological rock minerals, and accurately grasp the form of mineral combinations of geological rocks and the types of chemical elements, etc. [1, 2]. By a large number of investigations and analysis, it can be seen that the distribution and content of mineral

resources is not regular, and the variety of minerals is extremely large, commonly used in human life, including hydrochloric acid, oxygenated minerals, and the development of various fields of society on the demand for mineral resources is also great [3]. All these highlight the importance of geological rock mineral detection and analysis, which is related to the scientific and reasonable development and utilization of valuable mineral resources. However, how to improve the efficiency and utilization of mineral resources extraction is a problem that needs to be deeply explored at present [4, 5]. Therefore, in the process of research and use of rock mineral resources, it is especially critical to do a good job in the detection of trace elements of rock minerals.

1.1. **Related work.** Traditional methods for the determination of trace elements in rock minerals include spectrophotometry [6], atomic absorption spectrometry [7], and mass spectrometry [8]. Ajtony et al. [9] used graphite furnace atomic absorption for the determination of trace elements in rock minerals, which required drying and ashing procedures, and it took at least 1.5 min to analyze a sample. Rhodes et al. [10] used the reaction of metal element ions with specific complexes, but its practical application is less due to the difficulty of matching the relevant enzymes and complexes. Gouda et al. [11] used atomic absorption spectrometry (AAS) to detect trace elements in rock minerals, but chemical pre-treatment is required, which may cause secondary pollution. Inductively coupled plasma mass spectrometry (ICP-MS) technology has been widely used due to its high throughput, wide detection range and good precision. McInnes et al. [12] used ICP-MS to detect trace elements in rock minerals, and it took only 30 s to analyze one sample with a measurement range of $0.13 \sim 500$ ng/mL. Song et al. [13] conducted a study for the determination of nickel in rock minerals and separated different kinds of rock mineral components by ICP-MS standard mode with a Relative Standard Deviation (RSD) of 13.9%.

Although the trace elements determined in the above study are relatively comprehensive, they need to be determined and analyzed manually, and machine learning can automatically discover the patterns and laws in the data set and realize the automatic determination of mineral trace element species. Ramil et al. [14] detected and classified five kinds of mineral trace elements under polarized light microscope based on Artificial Neural Network (ANN) and proved that the best color space for mineral identification is RGB color space. Zhang et al. [15] based on multilayer perceptron to extract the characteristics of different kinds of rocks and convert them into numerical parameters as the input of the model to realize the category detection of rock minerals, but the detection efficiency is not high. Liu et al. [16] used the K-means clustering algorithm in machine learning to characterize the minerals analyzed by atomic absorption spectrometry based on the color characteristics of the minerals, and detected and assessed the trace elements of the rock minerals, but the detection was time-consuming. Bédard et al. [17] combined decision tree and Gene Expression Programming (GEP) methods to establish a trace element detection method for rock minerals, but the detection error is large. Ma and Huang [18] based on Convolutional Neural Network (CNN) to extract the features of minerals and the Mohs hardness of minerals to detect rock minerals, but the computational complexity is high.

Since neural network models are very easy to fall into local minima and slow to converge, Support Vector Machines (SVMs) are good at nonlinear regression estimation, and some scholars have adopted them for rock mineral detection. Zhang et al. [19] combined SVM with wavelet analysis and genetic algorithm to establish a more reliable detection model, with a detection accuracy of 87.5%. Sun et al. [20] combined atomic absorption spectroscopy and SVM to detect trace elements in minerals, and achieved good results.

Wang et al. [21] introduced LSTM to extract features of rocks and minerals, and realized the classification of trace elements by SVM, which improved the prediction accuracy of the model.

1.2. **Contribution.** Through the analysis of existing studies, it is known that the current rock mineral trace element detection method has redundant variables, which leads to poor detection effect. To address this problem, this paper proposes a trace element detection method for rock minerals based on ICP-MS and support vector machine, and the main work of this method is summarized as follows.

(1) The microwave digestion method was used to convert the rock samples into solution, and ICP-MS was used to directly determine the trace elements in the rock minerals, with scandium as the internal standard element to eliminate the matrix effect, and the correction equation was established to eliminate the polyatomic ionic interference produced by the oxide ions on the trace elements, so as to obtain the electrical signals of the trace elements.

(2) Denoising of electrical signals using the improved wavelet transform (WT), the improved wavelet packet denoising method corrects the misalignment of the signal frequency bands, and reconstructs the decomposed signals from the perspective of energy distribution, which is capable of not losing signal information in the high frequency bands, but also makes the signals free from noise interference in the low frequency bands.

(3) The Principal Component Analysis (PCA) algorithm is used to eliminate irrelevant signal variables and reduce the redundancy of the model. On this basis, the important signal features are extracted by using the multi-layer convolution of CNN, and the output features of each layer of CNN are fused and input into the SVM classifier improved by Harris Hawk Optimization (HHO) for detection.

(4) The experimental outcome implies that the detection accuracy of the proposed method is 95%, and the average absolute error is 0.1268, which not only improves the detection accuracy of trace elements, but also reduces the detection error, and provides a new way of thinking for the detection and analysis of trace elements in rock minerals.

2. Theoretical analysis.

2.1. **Principle of the ICP-MS method.** Mass spectrometry includes GC-MS, ICP-AES, ICP-MS and other methods, among which ICP-MS is widely used in the field of geological rocks and minerals analysis due to its multiple advantages such as high sensitivity, high precision and reproducibility, fast scanning and analyzing speed, and isotope analyzing ability. ICP-MS is an analytical instrument that combines ICP technology with mass spectrometry, where the ICP acts as an ion source and the mass spectrometer is a mass screening and analyzing instrument. The ICP-MS instrument consists of seven main components, including the injection system, the ICP ion source, the interface and ion optics, the mass analyzer, the multistage vacuum system, the detection and data processing system, and the computer system [22]. Of these, the injection system, ICP ion source, interface and lens, and mass analyzer are the core components, as shown in Figure 1.

The sample is ionized from the inlet system through the ion source ICP, forming an ion stream that enters the vacuum system through the interface. In the ion mirror, positive ions pass through normally and are focused, while negative ions, neutral particles and photons are intercepted. In the analyzer, the instrument changes the analyzer parameters to allow only the elemental ions with the required mass/charge ratio to pass through and enter the detector, where the number of ions entering is counted and the final elemental content is obtained from the intensity of the count.

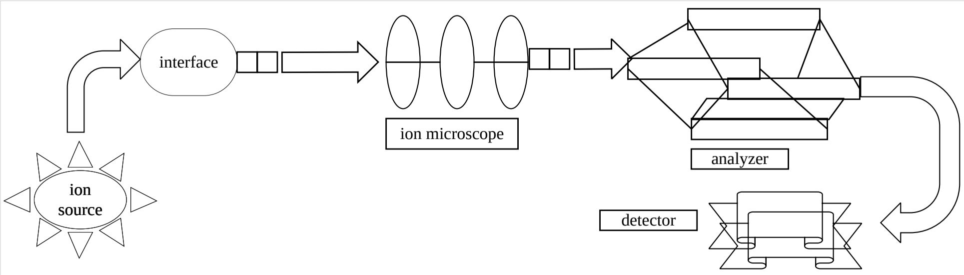

Figure 1. ICP-MS main component modules

2.2. **Support vector machine.** SVM is a widely used machine learning algorithm for classification and regression problems [23]. The advantage of SVM algorithm is that it has good generalization ability and performs well in the case of many features, while the disadvantage is that it is sensitive to noise. Compared with KNN, CNN and other algorithms, SVM can increase the computation speed while maintaining the accuracy rate. SVM constructs decision boundaries by searching for the support vectors closest to the samples of different categories, and then classifies the data in the test set to get the final result.

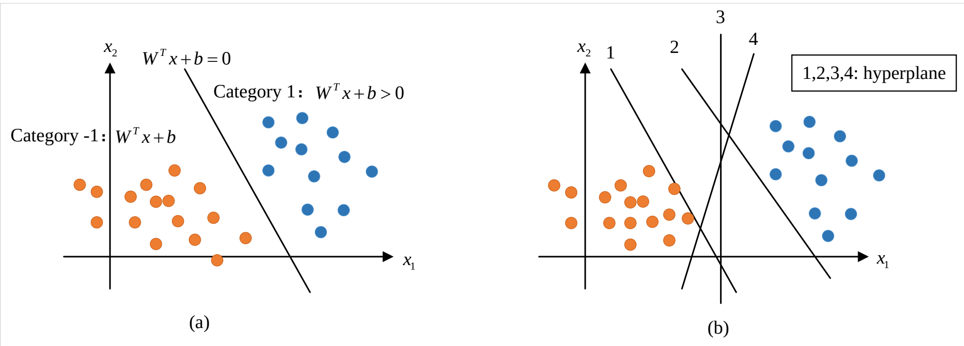

Figure 2. Schematic diagram of the SVM delineation plane

Let the dataset X contain N sample points $x_i \in R^K, i = 1, 2, ..., N$ in a K-dimensional space, and the corresponding class labels are denoted as $y_i \in \{-1, 1\}$, with -1 and 1 denoting the two classes. That is, $X = \{(x_1, y_1), \ldots, (x_N, y_N)\}$. There exists a hyperplane $w^T x + b = 0$ separating the two types of data, where w is a K-dimensional vector and b is a scalar. The SVM trains a hyperplane $w^T x + b = 0$ from X that can correctly classify the two types of data on each side of the hyperplane; this hyperplane is then used to classify the new data x_{new}, as shown in Figure 2, with the following decision function:

$$y_{new} = \mathrm{sign}(w^T x + b) \tag{1}$$

where sign is a sign function; b is a constant.

The aim of SVM is to seek an optimal separating hyperplane to minimize the classification error [24], defining the functional and geometric intervals as shown in Equation (2) and Equation (3), respectively.

$$l_i = y_i(w^T x + b) \tag{2}$$

$$r_i = \frac{1}{\|w\|} y_i(w^T x + b) \tag{3}$$

where y_i is the decision function, $w^T x + b$ is the hyperplane, and $\|w\|$ is the number of paradigms of w.

After defining the two intervals, the SVM binary classification task is transformed into an optimization problem: the parameters w and b are computed such that the geometric interval from the dataset to the hyperplane is maximized as shown in Equation (4), where r is either the functional interval or the geometric interval.

$$\max_{w,b} r \quad \text{s.t.} \frac{1}{\|w\|} y_i(w^T x + b) \geq r \tag{4}$$

3. **Trace element acquisition of geological rock minerals based on ICP-MS.** In view of the complex and time-consuming pre-treatment process of rock samples by ICP-MS, microwave digestion method [25] was adopted to efficiently transform rock samples into solution by using microwave energy, and trace elements in rock minerals were directly determined by ICP-MS, scandium was used as the internal standard element to eliminate matrix effects, and correction equations were established to eliminate the interference of oxide ions. Thus, electrical signals of trace elements can be obtained, and the specific process is shown in Figure 3.

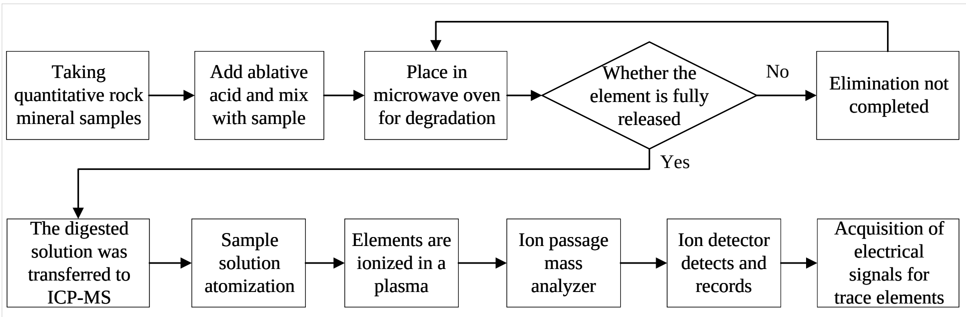

Figure 3. Specific flow of microwave digestion-ICP-MS

First, the microwave energy is used to convert the rock into a solution, the core equation of which is as follows. Where E is the energy of microwave, h is Planck's constant, and ν is the frequency of microwave.

$$E = h\nu \tag{5}$$

The rock is placed in a high-pressure, airtight microwave vessel with an appropriate amount of acid, and the microwave radiation rapidly heats the acid and the sample, resulting in a complete and rapid decomposition of the sample. Next, the resulting sample solution was introduced into the ICP-MS for analysis. The principle of ICP-MS is based on the ionization of ions in the sample solution by inductively coupled plasma (ICP), which generates cations and the concentration of each element by mass spectrometry (MS). The basic formula is as follows, where I is the intensity of the detected signal, C is the concentration of the rock sample, S is the sensitivity of the system, and E is the ionization efficiency of the element.

$$I = CSE \tag{6}$$

In this paper, scandium was chosen as the internal standard element, which has a moderate mass number and stable chemical properties, and is not easy to be chemically reacted or lost during sample handling and analysis. Since most of the trace elements in rocks are metallic elements with extremely complex compositions, in the process of ICP-MS, these interfering elements combine with O and Ar to produce interfering ions with the same isotopic masses as those of the trace elements, which seriously affects the accuracy of the measurement. Therefore, the deduction of the mass spectral interference is very important. By adding different amounts of the interfering elements Sr and Cu to the standard solutions of different concentrations of scandium, the final trace elements were measured, and the mass spectral interference correction formula was obtained as follows.

$$C = C_{Sc} - K_1 C_O - K_2 Ar \tag{7}$$

where C is the corrected elemental concentration, C_{Sc} is the apparent concentration of the measured Sc, K_1 and K_2 are the interference correction factors for the interfering elements.

The obtained trace element ion signals were converted into analyzable electrical signals using the calculation method proposed by Nishiguchi et al. [26] to obtain the final ICP-MS analyzed trace elements of the rock minerals as shown in Equation (8).

$$I = I_M - (I_E \times R) \tag{8}$$

where I is the corrected trace element determination, I_M is the sample containing the interfering element, I_E is the measured value of the interfering element, and R is the signal intensity ratio of the interfering element.

4. Trace element detection of rock minerals based on improved support vector machine.

4.1. Denoising of trace element electrical signals based on improved wavelet transforms. After obtaining the electrical signals of rock and mineral trace elements through ICP-MS, the improved wavelet transform (WT) is used to denoise the electrical signals, the redundant electrical signal variables are screened by PCA, and the main electrical signal features are extracted by the multi-layer convolution of CNN. HHO algorithm was used to find the optimal SVM hyperparameters to fit the relationship between trace element content and signal characteristics, and at the same time to complete the detection of trace elements in rocks and minerals, so as to solve the problem of low detection efficiency. The designed process of mineral trace element detection is shown in Figure 4.

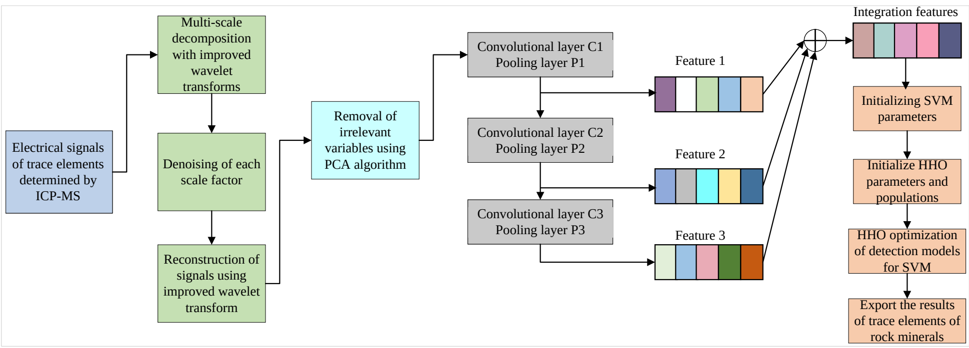

Figure 4. The designed process of mineral trace element detection

SVM classifiers are extremely sensitive to noise, and the commonly used denoising methods are Savitzky-Golay filter denoising and WT denoising [27], WT adopts a multi-resolution approach, which is able to portray the non-smooth features of the signal very well, so in this paper, we utilize WT for denoising of electrical signals of trace elements. Since the traditional WT for denoising is prone to frequency aliasing, in this paper, the signal to be analyzed is first convolved with the wavelet decomposition of the high-pass filter H and the low-pass filter G to obtain the convolved components. Then the C and D operations are performed to eliminate the excess frequency, and then the signal after zeroing is fast Fourier inverted and sampled at intervals, and the result of the sampling process is replaced by the result of the convolution. Finally the nodes are corrected to get the correct frequency band and eliminate the misalignment. Let $x(n)$ be the wavelet packet coefficients of the low-frequency subbands on the 2^j scale, then the formulas for C and D are shown below.

$$C = \begin{cases} X(k) = \sum_{n=0}^{N_j-1} x(n)W^{kn}, 0 \le k \le \frac{N_j}{4} \text{ or } \frac{3N_j}{4} \le k \le N_j \\ X(k) = 0, \text{other} \\ \tilde{x}(n) = \frac{1}{N_j}\sum_{n=0}^{N_j-1} x(k)W^{-kn} \end{cases} \tag{9}$$

$$D = \begin{cases} X(k) = \sum_{n=0}^{N_j-1} x(n)W^{kn}, \frac{N_j}{4} \le k \le \frac{3N_j}{4} \\ X(k) = 0, \text{other} \\ \tilde{x}(n) = \frac{1}{N_j}\sum_{n=0}^{N_j-1} x(k)W^{-kn} \end{cases} \tag{10}$$

where C and D are the operators that eliminate the excess band components after convolution with H and G in conventional WT, respectively, $W = e^{-j2\pi/N_j}$, N_j are the lengths of the data on the 2^j scale, D is the output of the operator, and $n = 0, 1, \dots, N_{j-1}$, $k = n = 0, 1, \dots, N_{j-1}$.

4.2. **Variable screening based on principal component analysis.** After WT denoising, a large number of variables in the trace element electrical signals were obtained, which also contained useless variables, so it was necessary to screen the feature data to eliminate irrelevant variables and reduce the redundancy of the model before subsequent analysis. Through PCA, the most important variables in the data are filtered out; the features that have the greatest impact on the data are prioritized for retention. This approach ensures that the main information in the data is maximized while removing redundant information. Assuming that there are m rock mineral trace elements and n signaling variables, which constitute the matrix $\chi_{m\times n} = (\chi_1, \chi_2, \dots, \chi_n)^T$, where $\chi_j = [\tau_{1j}, \tau_{2j}, \dots, \tau_{ij}, \dots, \tau_{mj}]^T$ consists of the original variables, let the new component after dimensionality reduction by PCA be $F_1, F_2, \dots, F_n$, i.e., $F_k = p_{k1}\chi_1 + p_{k2}\chi_2 + \dots + p_{kn}\chi_n$. The specific calculation steps are as follows.

The standardized initial evaluation matrix $\chi'_{mn} = (\tau'_{ij})_{m\times n}$ is first created, where τ'_{ij} is shown in Equation (11), and where $\bar{\tau}_j = 1/m\sum_{i=1}^m \tau_{ij}$, $s_j = \sqrt{\sum_{i=1}^m (\tau_{ij} - \bar{\tau}_j)^2/(m-1)}$.

$$\tau'_{ij} = \frac{\tau_{ij} - \bar{\tau}_j}{s_j} \tag{11}$$

Next, the matrix of correlation coefficients between the standardized variables, $R = (r_{jk})_{n\times n}$, is calculated as follows, where r_{jk} is the correlation coefficient between the j-th variable and the k-th variable.

$$r_{jk} = \frac{\sum_{i=1}^m (\tau_{ij} - \bar{\tau}_j)(\tau_{ik} - \bar{\tau}_k)}{\sqrt{\sum_{i=1}^m (\tau_{ij} - \bar{\tau}_j)^2 \sum_{i=1}^m (\tau_{ik} - \bar{\tau}_k)^2}} \tag{12}$$

After that, the eigenvalue $\lambda_1, \lambda_2, \dots, \lambda_n$ and its corresponding eigenvector $l_1, l_2, \dots, l_n$ of R were calculated, the principal component contribution ratio v_f and cumulative contribution ratio v_t were calculated, and the top f principal components with eigenvalue greater than 1 and cumulative contribution ratio more than 85% were selected as the final variables.

$$v_f = \frac{\lambda_f}{\sum_{k=1}^n \lambda_k} \tag{13}$$

$$v_t = \frac{\sum_{i=1}^t \lambda_i}{\sum_{k=1}^n \lambda_k} \tag{14}$$

where v_f is the contribution of the f-th principal component; v_t is the cumulative contribution of the first t principal components.

4.3. **Variable feature extraction based on convolutional neural network.** After removing the redundant variables, CNN is introduced for feature extraction of trace element signal variables, which has more powerful feature extraction capability compared to methods such as RNN and LSTM. CNN consists of input level, convolutional level, activation level, pooling level and fully connected level. In this paper, the sizes of CNN convolutional kernels are all set to 1×3 with a step size of 1. The numbers of convolutional kernels are 32, 64 and 128, respectively, and the sizes of maximal pooling layers are all set to 4×1 with a step size of 1, and a Relu activation function is set in each convolutional level.

The convolution level can automatically extract the local features of the spectral sample data, and the nonlinear activation function is introduced after the convolution to obtain the feature extraction results, as shown below:

$$g^i_{m,n} = f((J^i \times V)_{m,n}) + b_i \tag{15}$$

where V is the input matrix into the convolutional layer, $g^i_{m,n}$ is the output vector of the convolutional level in the m-th row and n-th column, J^i is the weight of the i-th convolutional kernel; b_i is the bias vector, and $f()$ is the activation function.

4.4. **Trace element detection of rock minerals based on Harris Hawk optimized SVM.** In SVM, the larger the penalty parameter C and the kernel function parameter g are, the higher the dimensionality of the mapping is, the better the training results are, but the possibility of overfitting is also greater. Therefore, it is necessary to choose the most suitable parameters to construct the SVM classifier. In this paper, HHO [28] is used to search for the optimal hyperparameters of SVM for optimal detection. HHO achieves population evolution by mathematically modeling different feeding strategies of Harris's hawk. The whole optimization process includes three stages: exploration, conversion between exploration and development, and development. Compared with heuristic algorithms such as PSO and GA, this algorithm has the advantages of simple principle, no cumbersome parameter tuning, and excellent global search capability, etc. The specific steps are as follows.

(1) Initialize the parameters of the HHO algorithm, including the population size of Harris's hawk and the maximum number of iterations. Then a set of initial positions of Harris's Hawk (HH) is randomly generated, and in the exploration phase, a random number q is generated for each position based on the value of q. $q < 0.5$ is the distance between the positions of Harris's hawk close to the prey, and $q \geq 0.5$ is the random position between the HHs.

$$X(t+1) = \begin{cases} X_{rand}(t) - r_1|X_{rand}(t) - 2r_2X(t)| & q \geq 0.5 \\ (X_{rabbit}(t) - X_m(t)) - r_3(LB + r_4(UB - LB)) & q < 0.5 \end{cases} \tag{16}$$

where t is the current iteration; $X(t+1)$ is the position vector of the next iteration; $X_{rand}(t)$ is the position of a random individual in the flock; $X_{rabbit}(t)$ is the position vector of the rabbit to be hunted; UB and LB are the upper and lower bounds of the search space, respectively; r_1, r_2, r_3, and r_4 are random numbers; and $X(t)$ is the current position vector.

(2) The Root Mean Square Error (RMSE) of the SVM is used as the fitness function, and then the fitness value of each HH is calculated. The location of the HH with the best

fitness value is taken as the global optimal solution as follows.

$$R_{RMSE} = \sqrt{\frac{1}{r}\sum_{p=1}^{r}(y_p - y)^2} \tag{17}$$

$$g_{best} = X_{rabbit}(t) - R_{RMSE}|JX_{rabbit}(t) - X_m(t)| \tag{18}$$

where y_p is the predicted value, y is the actual value, and J is the strength of the rabbit's random jumps.

(3) Calculate the fitness value and use the optimized SVM for rock mineral trace element detection. If the fitness value of the updated HH is better than the current g_{best}, g_{best} will be replaced by that fitness value, and when the maximum number of iterations is exceeded, the optimal parameters C and g of the search SVM are outputted, thus mapping the unsolvable nonlinear problem in the low-dimensional space to the high-dimensional space through the kernel function, thus simplifying the optimal separating hyperplane solution as follows.

$$f(g_i) = w \cdot \phi(g_i) + b \tag{19}$$

where w, b are the weight vector and threshold, respectively; g is the extracted trace element feature.

For a given training dataset $\{(g_i, y_i), i = 1, 2, \ldots, n\}$, the constrained optimization problem is expressed as follows by using the insensitive loss function ϵ to process the weights w and thresholds b to be sought in the detection model through the principle of structural risk minimization.

$$\min \frac{1}{2}\|w\|^2 + C\sum_{i=1}^{n}(\xi_i + \xi_i^*) \quad s.t. \begin{cases} y_i - w \cdot \phi(x) - b \le \epsilon + \xi_i \\ w \cdot \phi(x) + b - y_i \le \epsilon + \xi_i^* \\ \xi_i, \xi_i^* \ge 0 \end{cases} \tag{20}$$

where C is the penalty parameter after HHO optimization, which determines how well the function fits, and as C becomes larger, it is necessary to make the model less tolerant to detection errors, and thus C is related to the generalization ability of SVM. ξ_i and ξ_i^* are non-relaxation variables, and ϵ is used to measure the deviation of the training samples outside the insensitive region.

In addition, the optimization problem is transformed into a dyadic problem by introducing the Lagrangian function, and finally the decision function of SVM is obtained by introducing the optimal kernel function as follows.

$$f(x) = \sum_{i=1}^{n_{sv}}(a_i - a_i^*)K(x_i, x) + b \tag{21}$$

where n_{sv} is the number of support vectors.

5. Performance testing and analysis.

5.1. Analysis of precision experimental results of the ICP-MS method. In this paper, the data of 105 geological rock mineral trace elements from the literature [29] are utilized as a dataset, which contains the concentration data of iron, manganese, copper, zinc, lead, nickel and other trace elements as well as the electrical signal data, which are classified in this paper as pro-ferrous, pro-copper, pro-gas, and pro-manganese, and are labeled as 1, 2, 3, and 4, respectively. The dataset is divided into training and test sets in the ratio of 8 : 2, and 10% of the samples from the training set are used as the validation set. The experimental platform is Ubuntu 18.04.5 operating system, the graphics card is NVIDIA RTX 1650Ti, and the software environment is Python 3.6.0 and Tensorflow

2.0. All models were cross-validated using 10-fold cross validation, setting the epoch to 5000 rounds and the batch size to 32, and the network was updated by using the Adam optimization method.

By analyzing the trace element contents in the dataset, a box-and-line diagram of the major trace element contents in geological rock minerals can be obtained as shown in Figure 5. The Mn content ranged from 9.94% to 42.4% with an intermediate value of 21%, and the Fe content ranged from 23.4% to 63.2% with an intermediate value of 47.4%. The Cu content ranges from 9.94% to 45.6%. The Pb content is relatively small, ranging from 3.5% to 9.79%, with an intermediate value of 6.1%, so that the main trace elements in geological rock minerals are Fe, Mn, Cu, Zn and Pb.

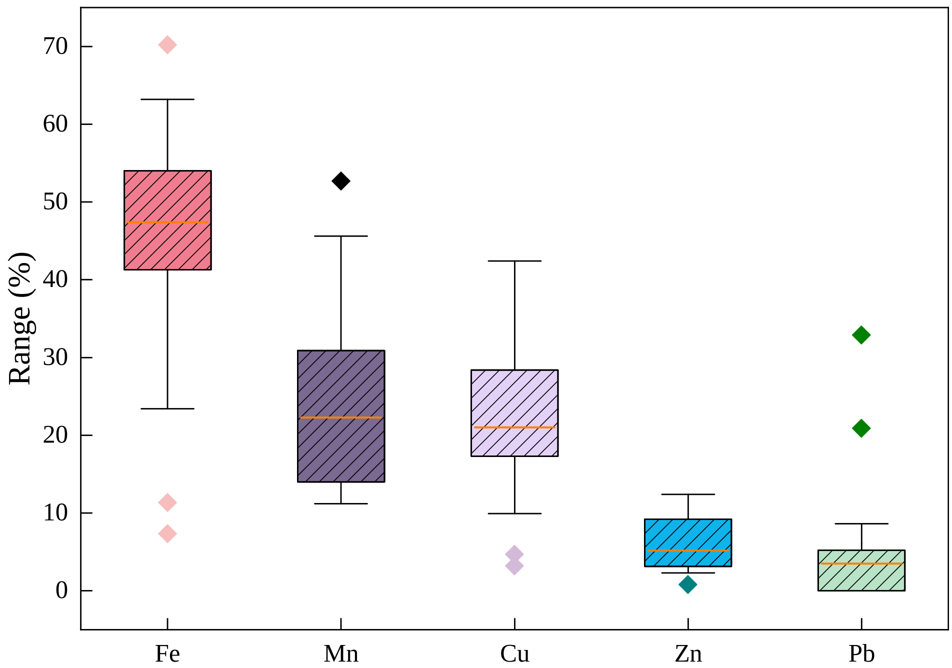

Figure 5. The major trace element contents in geological rock minerals

After analyzing the major trace elements, the proposed microwave ICP-MS (MCICP-MS) was compared with spectrophotometry (SPM) and atomic absorption spectrometry (AAS) for comparison experiments. Comparison of the results of the precision experiments of the different methods for the major trace elements are shown in Table 1. where RE stands for relative error and RSD stands for relative standard deviation. Overall, the RE of ICP-ESVM results to the determined values was -7.8% $\sim$ 9.8%, and the RSD was not more than 9.6%, which was higher compared to both SPM and AAS, and fully verified the high efficiency of the introduction of MCICP-MS.

5.2. **Performance analysis of trace element assay for rock minerals.** To verify the detection effect of the proposed detection method MCICP-MS, MCICP-MS was compared with RM-MLP [15], WT-SVM [19], and LSTM-SVM [21] in the comparison experiments, and the results of the different methods for the detection of trace elements in rock minerals are shown in Figure 6. In Figure 6 (d), the detection accuracy of MCICP-MS was 95%, which was improved by 5%, 7.5%, and 12.5% compared with RM-MLP in Figure 6 (a), WT-SVM in Figure 6 (b), and LSTM-SVM in Figure 6 (c), respectively. MCICP-MS not only efficiently analyzes trace element signal variables using ICP, but also reduces

Table 1. Analysis of precision experimental results of different methods

Trace element	SPM		AAS		MCICP-MS	
	RE/%	RSD/%	RE/%	RSD/%	RE/%	RSD/%
Fe	3.4	7.3	1.8	5.2	1.3	3.9
Mn	5.1	8.9	3.9	7.1	3.0	6.4
Cu	8.2	6.4	6.5	5.7	5.3	4.6
Zn	7.1	5.6	5.1	4.8	3.9	4.3
Pb	13.8	8.7	11.2	7.5	9.8	6.8

the complexity of input variables by screening redundant variables using PCA. Furthermore, MCICP-MS utilizes HHO to search for the optimal hyperparameters of SVM, which improves the effectiveness of detection.

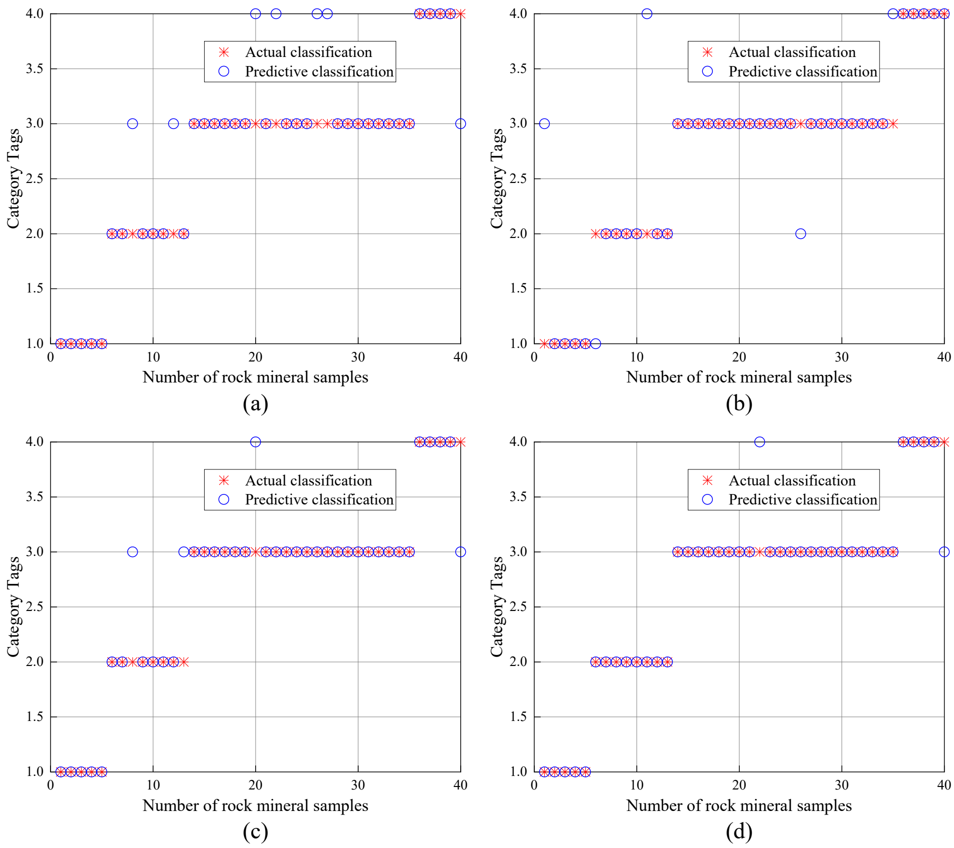

Figure 6. The results of the different methods for the detection of trace elements

In addition to analyzing the accuracy of detection, this paper also utilizes the detection performance metrics RMSE, MAE, and R^2 which also need to be further analyzed for detection accuracy as shown in Table 2. The closer the R^2 is to 1, the higher the correlation between the independent variable and the dependent variable. It is usually considered that the model with $R^2 > 0.5$ has good detection effect, and the R^2 of all four models is greater than 0.5, so all four models are valid, and the R^2 of MCICP-MS is 0.9863, which shows the best detection effect. Furthermore, the RMSE and MAE of MCICP-MS were reduced by at least 17.45% compared with RM-MLP, WT-SVM, and LSTM-SVM, and

RM-MLP detected trace elements by MLP, but redundant variables were not eliminated, so the detection efficiency was not high. WT-SVM did not extract the features of trace elements and only used the unoptimized SVM for trace element classification, so the detection efficiency is not as good as LSTM-SVM and MCICP-MS. The LSTM-SVM did not consider the screening of non-critical variables and did not sufficiently extract the main features of trace elements, so that the best detection performance of MCICP-MS using ICP-MS and improved SVM was obtained.

Table 2. Comparison of detection accuracy of different detection methods

Model	RMSE	MAE	R^2
RM-MLP	0.1459	0.2154	0.8819
WT-SVM	0.1184	0.1971	0.9056
LSTM-SVM	0.0940	0.1586	0.9364
MCICP-MS	0.0776	0.1268	0.9863

6. **Conclusion.** As the basic elements of the earth system, rock minerals play an important role in geoscience and mineral resources exploration. This paper addresses the problem that the existing trace element detection methods for rock minerals ignore important variables, resulting in unsatisfactory detection results. Firstly, the rock samples were converted into solution by microwave digestion, and the trace elements in the rock minerals were directly determined by ICP-MS, and the corrective equations were established to eliminate the polyatomic ion interference produced by the oxide ions on the trace elements, and to obtain the electrical signals of the trace elements. Then the improved WT is used to denoise the electrical signals, the PCA algorithm is introduced to eliminate the irrelevant variables in the denoised electrical signals, and the important signal features are extracted by using the multi-layer convolution of CNN, and the output features of each layer in the middle of CNN are fused and inputted into the improved SVM classifier of HHO for detection. The experimental outcome indicates that the detection accuracy of the offered approach has been improved by at least 5%, and the detection error has been reduced by at least 17.45%, which has higher detection accuracy and precision, and can better realize the detection of trace elements in rock minerals. There are many kinds of minerals in rocks, this paper only for the main trace elements for experimental analysis, for the content of lesser mineral elements due to the lack of samples in the dataset, data labeling difficulties, etc., in the subsequent research needs more comprehensive mineral library and more accurate mineral detection algorithms to make the model more versatile.

REFERENCES

[1] Y. Zhang, L. Zhang, Y. Chang, Z. Fan, and D. Guo, "Determining trace elements in rock samples containing refractory minerals by pressurize-microwave inductively coupled plasma mass spectrometry," *Uranium Geology,* vol. 34, no. 2, pp. 105–111, 2018.

[2] M. Mao, A. S. Rukhlov, S. M. Rowins, J. Spence, and L. A. Coogan, "Apatite trace element compositions: A robust new tool for mineral exploration," *Economic Geology,* vol. 111, no. 5, pp. 1187–1222, 2016.

[3] T.-Y. Wu, H. Li, and S.-C. Chu, "CPPE: An Improved Phasmatodea Population Evolution Algorithm with Chaotic Maps," *Mathematics,* vol. 11, no. 9, p. 1977, 2023.

[4] T.-Y. Wu, H. Li, S. Kumari, and C.-M. Chen, "A Spectral Convolutional Neural Network Model Based on Adaptive Fick's Law for Hyperspectral Image Classification," *Computers, Materials & Continua,* vol. 79, no. 1, pp. 19–46, 2024.

[5] T.-Y. Wu, A. Shao, and J.-S. Pan, "CTOA: Toward a Chaotic-Based Tumbleweed Optimization Algorithm," *Mathematics,* vol. 11, no. 10, p. 2339, 2023.

[6] A. Shah, F. Sikandar, I. Ullah, A. Shah, S. Ud-Din Khan, U. Usman Ali Rana, and T. McCoy, "Spectrophotometric determination of trace elements in various honey samples, collected from different environments," *Journal of Food and Nutrition Research,* vol. 2, no. 9, pp. 532–538, 2014.

[7] A. Gouda, R. El Sheikh, H. El Sayed, A. Khedr, S. A. Al Ezz, W. Gamil, and M. Hamdy, "Ultrasound-assisted dispersive microsolid-phase extraction for preconcentration of trace cobalt and nickel in environmental samples prior to their determination by flame atomic absorption spectrometry," *Journal of Applied Spectroscopy,* vol. 89, no. 3, pp. 567–578, 2022.

[8] L. Zhang, Z. Y. Ren, X. P. Xia, Q. Yang, L. B. Hong, and D. Wu, "In situ determination of trace elements in melt inclusions using laser ablation inductively coupled plasma sector field mass spectrometry," *Rapid Communications in Mass Spectrometry,* vol. 33, no. 4, pp. 361–370, 2019.

[9] Z. Ajtony, L. Bencs, R. Haraszi, J. Szigeti, and N. Szoboszlai, "Study on the simultaneous determination of some essential and toxic trace elements in honey by multi-element graphite furnace atomic absorption spectrometry," *Talanta,* vol. 71, no. 2, pp. 683–690, 2007.

[10] R. H. Rhodes, J. A. Baker, M.-A. Millet, and N. A. Bertler, "Experimental investigation of the effects of mineral dust on the reproducibility and accuracy of ice core trace element analyses," *Chemical Geology,* vol. 286, no. 3-4, pp. 207–221, 2011.

[11] A. Gouda, R. El Sheikh, H. El Sayed, A. Khedr, S. A. Al Ezz, W. Gamil, and M. Hamdy, "Ultrasound-assisted dispersive microsolid-phase extraction for preconcentration of trace cobalt and nickel in environmental samples prior to their determination by flame atomic absorption spectrometry," *Journal of Applied Spectroscopy,* vol. 89, no. 3, pp. 567–578, 2022.

[12] M. McInnes, J. D. Greenough, B. J. Fryer, and R. Wells, "Trace elements in native gold by solution ICP-MS and their use in mineral exploration: A British Columbia example," *Applied Geochemistry,* vol. 23, no. 5, pp. 1076–1085, 2008.

[13] X. Song, J. Lai, J. Xu, X. Liu, B. Li, H. He, Y. Wang, J. Shi, C. Wang, and C. Wen, "Material Source and Genesis of the Daocaowan Sb Deposit in the Xikuangshan Ore Field: LA-ICP-MS Trace Elements and Sulfur Isotope Evidence from Stibnite," *Minerals,* vol. 12, no. 11, p. 1407, 2022.

[14] A. Ramil, A. López, J. S. Pozo-Antonio, and T. Rivas, "A computer vision system for identification of granite-forming minerals based on RGB data and artificial neural networks," *Measurement,* vol. 117, pp. 90–95, 2018.

[15] Y. Zhang, M. Li, S. Han, Q. Ren, and J. Shi, "Intelligent identification for rock-mineral microscopic images using ensemble machine learning algorithms," *Sensors,* vol. 19, no. 18, p. 3914, 2019.

[16] C. Liu, M. Li, Y. Zhang, S. Han, and Y. Zhu, "An enhanced rock mineral recognition method integrating a deep learning model and clustering algorithm," *Minerals,* vol. 9, no. 9, p. 516, 2019.

[17] É. Bédard, V. D. B. de Vazelhes, and G. Beaudoin, "Performance of predictive supervised classification models of trace elements in magnetite for mineral exploration," *Journal of Geochemical Exploration,* vol. 236, p. 106959, 2022.

[18] S. Ma, and W. Huang, "Application of Deep Learning Algorithms in Determination of Trace Rare Earth Elements of Cerium Group in Rocks and Minerals," *Wireless Communications and Mobile Computing,* vol. 1, pp. 1–10, 2021.

[19] P. Zhang, Z. Zhang, J. Yang, and Q. Cheng, "Machine learning prediction of ore deposit genetic type using magnetite geochemistry," *Natural Resources Research,* vol. 32, no. 1, pp. 99–116, 2023.

[20] G. Sun, Q. Zeng, and J.-X. Zhou, "Machine learning coupled with mineral geochemistry reveals the origin of ore deposits," *Ore Geology Reviews,* vol. 142, p. 104753, 2022.

[21] L. Wang, C. Zhang, R. Geng, Y. Li, J. Song, B. Wang, and F. Cui, "The discrimination of tectonic settings using trace elements in magmatic zircons: A machine learning approach," *Earth Science Informatics,* vol. 16, no. 4, pp. 4097–4112, 2023.

[22] B. Meermann, and V. Nischwitz, "ICP-MS for the analysis at the nanoscale–a tutorial review," *Journal of Analytical Atomic Spectrometry,* vol. 33, no. 9, pp. 1432–1468, 2018.

[23] A. Pradhan, "Support vector machine-a survey," *International Journal of Emerging Technology and Advanced Engineering,* vol. 2, no. 8, pp. 82–85, 2012.

[24] J. Cervantes, F. Garcia-Lamont, L. Rodríguez-Mazahua, and A. Lopez, "A comprehensive survey on support vector machine classification: Applications, challenges and trends," *Neurocomputing,* vol. 408, pp. 189–215, 2020.

[25] S. Kopru, M. Cadir, and M. Soylak, "Investigation of trace elements in vegan foods by ICP-MS after microwave digestion," *Biological Trace Element Research,* vol. 200, no. 12, pp. 5298–5306, 2022.

[26] K. Nishiguchi, K. Utani, and E. Fujimori, "Real-time multielement monitoring of airborne particulate matter using ICP-MS instrument equipped with gas converter apparatus," *Journal of Analytical Atomic Spectrometry,* vol. 23, no. 8, pp. 1125–1129, 2008.

[27] M. Grobbelaar, S. Phadikar, E. Ghaderpour, A. F. Struck, N. Sinha, R. Ghosh, and M. Z. I. Ahmed, "A survey on denoising techniques of electroencephalogram signals using wavelet transform," *Signals,* vol. 3, no. 3, pp. 577–586, 2022.

[28] A. A. Heidari, S. Mirjalili, H. Faris, I. Aljarah, M. Mafarja, and H. Chen, "Harris hawks optimization: Algorithm and applications," *Future Generation Computer Systems,* vol. 97, pp. 849–872, 2019.

[29] É. Bédard, V. D. B. de Vazelhes, and G. Beaudoin, "Performance of predictive supervised classification models of trace elements in magnetite for mineral exploration," *Journal of Geochemical Exploration,* vol. 236, p. 106959, 2022.